This document was prepared in conjunction with work accomplished under Contract No. DE-AC09-96SR18500 with the U. S. Department of Energy.

DISCLAIMER

This report was prepared as an account of work sponsored by an agency of the United States Government. Neither the United States Government nor any agency thereof, nor any of their employees, nor any of their contractors, subcontractors or their employees, makes any warranty, express or implied, or assumes any legal liability or responsibility for the accuracy, completeness, or any third party's use or the results of such use of any information, apparatus, product, or process disclosed, or represents that its use would not infringe privately owned rights. Reference herein to any specific commercial product, process, or service by trade name, trademark, manufacturer, or otherwise, does not necessarily constitute or imply its endorsement, recommendation, or favoring by the United States Government or any agency thereof or its contractors or subcontractors. The views and opinions of authors expressed herein do not necessarily state or reflect those of the United States Government or any agency thereof.

CRACK TIP OPENING DISPLACEMENT AND ANGLE FOR A GROWING CRACK IN CARBON STEEL

Poh-Sang Lam
Savannah River National Laboratory, Aiken, SC 29808

Yil Kim, and Yuh J. Chao
Department of Mechanical Engineering, University of South Carolina, Columbia, SC 29208

ABSTRACT

The crack tip opening displacements and angles (CTOD/CTOA) are calculated with finite element method based on the test data of a set of constraint-dependent J-R curves for A285 carbon steel. The values of the CTOD/CTOA are initially high at initiation, but rapidly decrease to a nearly constant value. When the common practice is adopted by using only the constant part of CTOD/CTOA as the fracture criterion, the crack growth behavior is shown to be severely underestimated. However, with a bilinear form of CTOD/CTOA fracture criterion which approximates the initial non-constant portion, the experimental load vs. crack extension curves can be closely predicted. Furthermore, it is demonstrated that the CTOD/CTOA is crack tip constraint dependent. The values of CTOD/CTOA for specimens with various ratios of crack length to specimen width (a/W) are reflected by the J-R curves and their slopes.

INTRODUCTION

As an alternative fracture criterion based on the stress intensity factor or J-integral, the directly measurable quantities such as the crack tip opening displacement and/or angle (CTOD/CTOA) have gain much attention in recent years when the advance in measurement technologies allows accurate measurement of these fracture parameters, such as the optical microscopy (e.g., [1]), digital image correlation (e.g., [2,3]) and microtopography [4], etc. In addition, the development in high speed computation leads to realistic virtue simulation of fracture testing to extract these quantities at any length scale and in three-dimensional space. The combination of experimental and numerical methods indeed provides insight to the true fracture mechanisms in materials. In this paper, the CTOD is defined as the crack opening displacement (δ) measured at a fixed distance (x) behind the current crack tip, and CTOA= $2\tan^{-1}[\delta/(2x)]$. Since CTOD and CTOA are equivalent, where appropriate, the term CTOD is understood to refer also to CTOA throughout the paper, unless it is specifically pointed out

A comprehensive review of the work on CTOD can be found in Newman, et al. [5]. The majority of the test data (e.g., aluminum alloys and A533B) and the numerical analyses (e.g., [1,6-19]) seem to indicate that the values of CTOD are initially high, but

progressively decrease to a nearly constant value after several millimeters of crack growth. It has been shown by several investigators (e.g., [9-11,15,20-23]) that, based on three-dimensional (3D) and two-dimensional (2D) finite element analyses, a *constant* CTOD fracture criterion may be capable of predicting the experimental data (e.g., load versus crack extension curves). This leads to a speculation that the initial high values of CTOD may be a result of inadequacy of the measurement technique on the specimen surface; while crack tunneling, shear lips or slant fracture may have occurred during the test in specimens including compact tension (CT) and middle-cracked tension (MT).

The finite element analysis with nodal release algorithm [24] is used to simulate a growing crack based on the test data from a set of single edge-notched bend (SENB) specimens, which were tested previously for developing a constraint-modified J-R curve [25] for A285 Grade C carbon steel, using the J-A_2 two-parameter constraint theory of fracture for elastic-plastic materials [26-28]. The post-test fractography indicated that the crack front was straight and the deformation seemed to be plane strain. As a result, one of the specimens is verified with a three-dimensional finite element analysis (3D-FEA), and the result is demonstrated to be equivalent to the corresponding two-dimensional finite element analysis (2D-FEA). Both the experimental J-R curve and the load-displacement curve for the specimen can be reproduced by the finite element procedure.

A constant CTOD criterion is first employed to predict crack growth in these specimens but the results show a severe under-estimation of both of the J-R and the load-displacement curves. On the other hand, the use of a bilinear form of CTOD to account for its initial high values, a very good agreement between the experimental and predicted curves can be achieved. This implies that the initial values of CTOD contain the essential information and momentum to drive the crack to a steady state which can indeed be characterized by a constant CTOD growth criterion. The characteristics of the initial values of CTOD have been recognized earlier by Kanninen et al [29]. As pointed out in Kanninen and Popelar (Fig. 5.58 in [30]), the use of a constant CTOA as the fracture criterion would underestimate the fracture load.

Finally, using the experimental J-R curves in Lam et al. [25] and following the derivations in Kanninen and Popelar [30] and in Gullerud et al. [16], the CTOD is qualitatively proportional to the slope of the J-R curve, and the initial high values of CTOD is shown to be a natural consequence of the crack growth resistance. Since the J-R curve is strongly depend on a/W, it can then be concluded that CTOD is essentially a function of crack tip in-plane constraint.

EXPERIMENTS

The material under investigation is A285 carbon steel Grade C, heat E400 plate with 0.18 wt.% carbon, 0.43 wt.% manganese, and 0.026 wt.% sulfur. The tensile test shows that the 0.2% offset yield stress (σ_o) is 251 MPa (36.4 ksi), the ultimate tensile stress 415 MPa (60.2 ksi), the flow stress (σ_f) 333 MPa (48.3 ksi, defined as the average of the 0.2% yield stress and the ultimate stress), and the Young's modulus (E) 207 GPa (30,000 ksi).

The Poisson ratio of the material is 0.3. The true stress-true strain curve is shown in Figure 1. The stress-strain curve can be expressed as a Ramberg-Osgood power law:

$$\frac{\varepsilon}{\varepsilon_o} = \frac{\sigma}{\sigma_o} + 3.2\left(\frac{\sigma}{\sigma_o}\right)^5$$

where $\varepsilon_o = \sigma_o/E$.

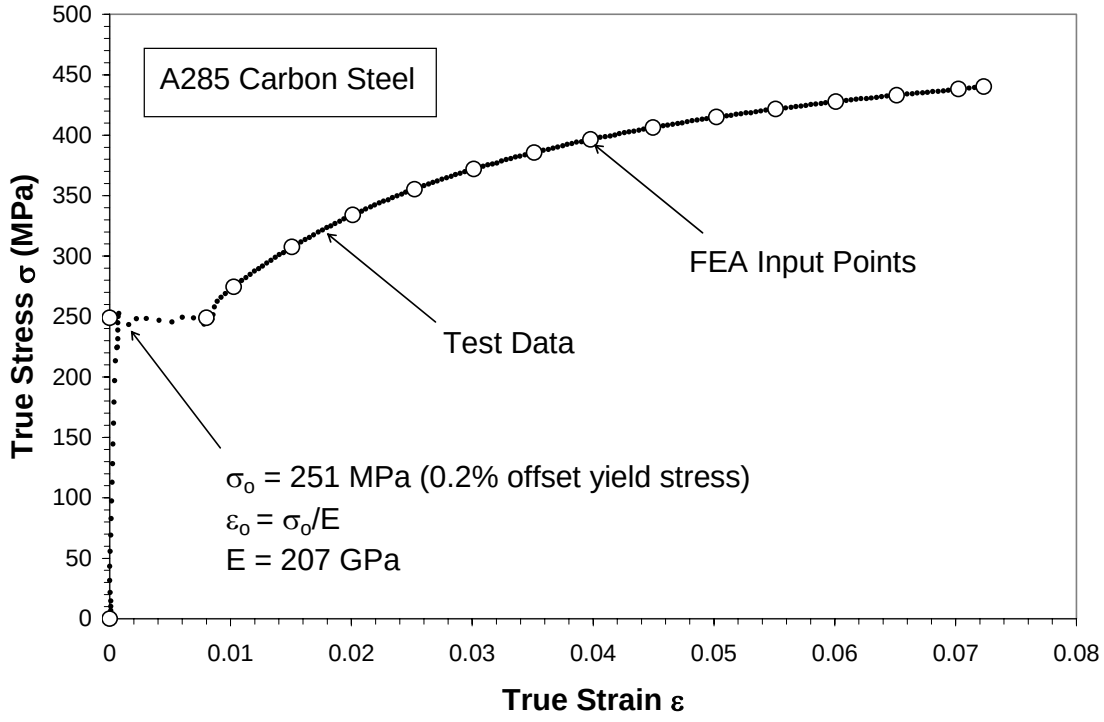

Figure 1 True stress-true strain curve for A285 Grade C heat 400 plate.

The SENB specimens were fabricated in accordance with the specifications in the American Society for Testing and Materials (ASTM) "Standard Test Method for Measurement of Fracture Toughness" (E 1820), except for the initial crack lengths that were varied to achieve different a/W or different levels of crack tip constraint. The specimen thickness B is 15.875 mm (0.625 inches) with 10% side groove on each side (net thickness B_N is 12.7 mm or 0.5 inches), the width W is 31.75 mm (1.25 inches), the length L is 142.88 mm (5.625 inches), and the span S is 127 mm (5 inches). After fatigue cracking, the initial crack depth to the width ratios (a/W) for the fracture toughness test specimens are, respectively, 0.32 (Specimen 1D), 0.59 (Specimen 2A), and 0.71 (Specimen 4C). These specimens were originally used to develop a constraint-modified J-R curve for A285 carbon steel storage tanks [25]. The same set of test data are used in the current study of CTOD during the course of crack extension in this paper.

The guidelines provided by the ASTM E1820 were used to conduct the SENB fracture toughness testing. The post-test fractography shows that the crack fronts are mostly straight with a slightly reversed thumbnail formed near the edges because of the presence of side grooves. The experimental J-R data are plotted in Figure 2, which clearly shows a distinct specimen size-dependent, in-plane constraint effect. It is intended in this paper to demonstrate that the crack tip constraint influences the CTOD during crack growth, and therefore any CTOD-based fracture criteria. Also included in Figure 2 are the finite element predictions of the J-R curves, which will be discussed later in the paper.

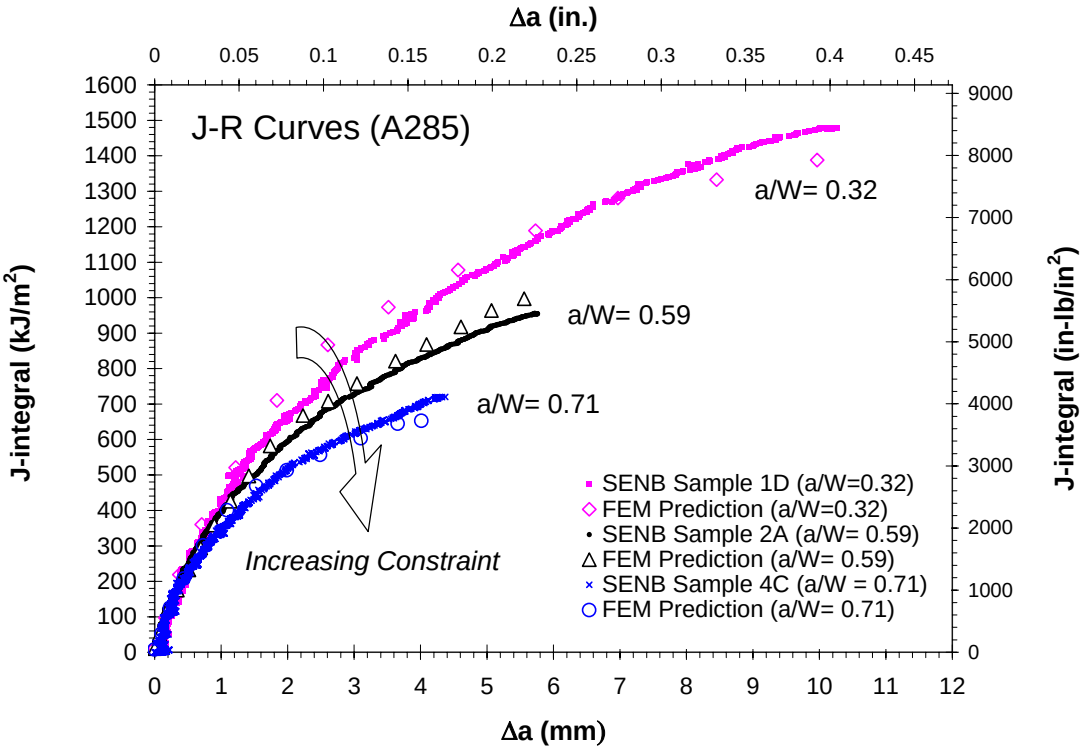

Figure 2 Experimental J-R curves with in-plane crack tip constraint.

THREE-DIMENSIONAL FINITE ELEMENT ANALYSIS

The configuration of Specimen No. 2A (a/W= 0.59) was selected for 3D-FEA of the J-integral fracture testing. The 3D-FEA result is used as a benchmark for the subsequent 2D-FEA. Because of symmetry, only one quarter of the SENB specimen is modeled (Fig. 3). This model includes a 10% side groove (each side) and uses 35970 eight-node, reduced integration brick elements with 41684 nodes. To facilitate the crack growth simulation, very fine and uniformly spaced elements are arranged in the crack tip region. The general purpose finite element program ABAQUS [24] was used for calculation. The elastic-plastic analysis was carried out with the full stress-strain curve input as shown in Figure 1. Incremental plasticity is assumed for the material response above the

yield point, and a finite deformation formulation is invoked. The loading pin movement is imposed as a prescribed nodal displacement.

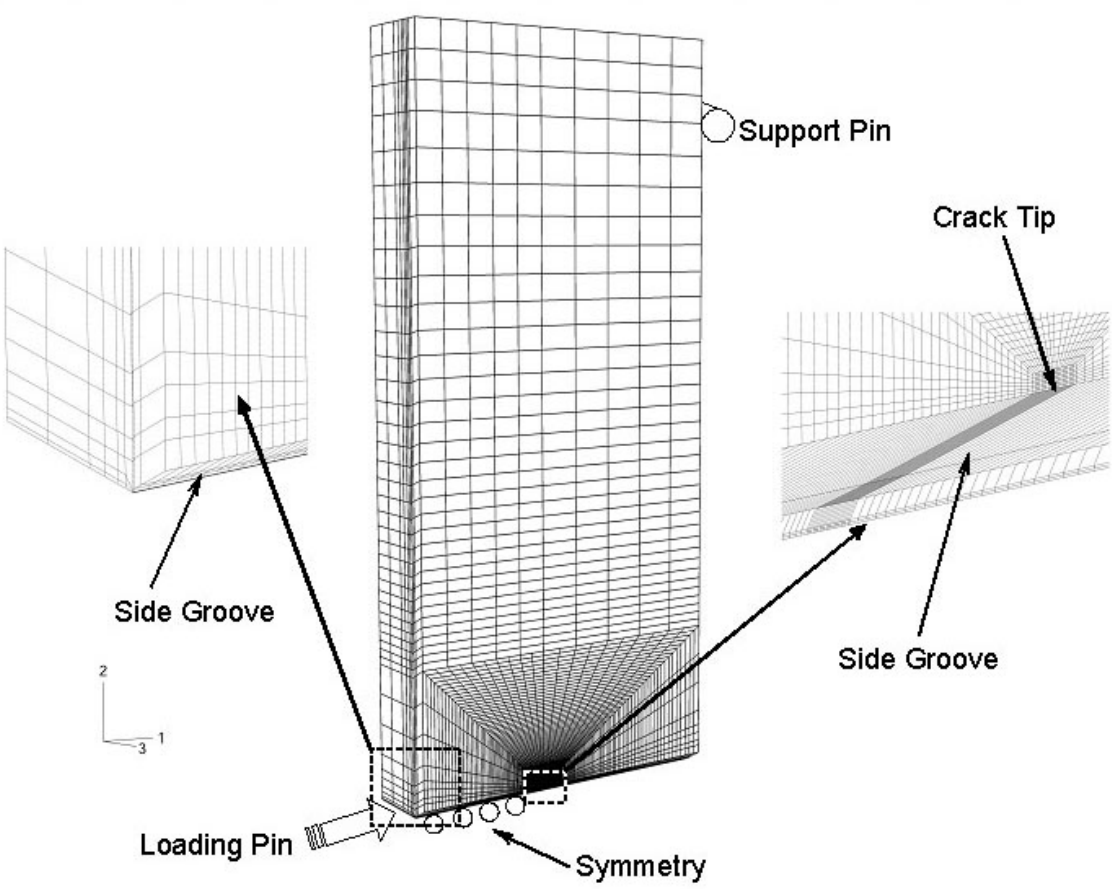

Figure 3 Three-dimensional finite element model of the SENB specimen with a/W=0.59.

The ABAQUS nodal release capability is utilized to model the growing crack during the fracture toughness test. The crack growth criterion is the crack length vs. load point displacement test data. Based on the nearly straight crack front on the fracture surface, it is not unreasonable to assume that the crack front remains straight during the course of crack extension throughout the test. As a result, the finite elements nodes immediately ahead of the current (straight) crack front nodes are released simultaneously when the crack growth condition is met.

The calculated load-displacement curve at the loading point is compared with the corresponding experimental curve. The good agreement indicates that the crack extension simulation is adequate.

TWO-DIMENSIONAL FINITE ELEMENT ANALYSIS

A 2D-FEA is performed for the same case of a/W=0.59. The goal is to demonstrate that the equivalent CTOD solution can be obtained from the two-dimensional analysis.

This finite element model contains 13072 four-node reduced integration plane strain elements with 13635 nodes. A very fine mesh with square elements is populated in the anticipated crack growth region which extends to the edge of the specimen in order to facilitate the J-integral evaluation under potentially large scale yielding and extensive crack growth. The same tensile properties as shown in Figure 1 are used. Similar to the 3D-FEA, the crack tip nodes are released following the crack growth criterion set by the crack length vs. load point displacement test data. Note that in the 3D-FEA, the entire row of finite element nodes ahead of the current crack front are released simultaneously, while in the 2D-FEA, the crack growth is simulated by releasing one node at a time ahead of the present crack tip.

As in the case of 3D-FEA, the load-displacement curve predicted by 2D-FEA is compared with the experimental data. Very good agreement was again achieved and the adequacy of the analysis is established.

FINITE ELEMENT RESULTS OF a/W=0.59

Figure 4 shows the calculated CTOA of the specimen at various amount of crack growth (Δa). It can be seen that the CTOA distribution is not sensitive across the thickness t, where z=0 represents the mid-thickness of the plate, and z= 0.5t is the plane at the root of the side groove. These CTOA values are measured at 1 mm behind the crack tip, as commonly chosen by some researchers [5,16,31]. The result of an equivalent plane strain finite element analysis is also plotted in Figure 4. Because the flat crack front revealed in the post-test fractography and the results shown in Figure 4, it may be concluded that the 2D-FEA is sufficient for this specimen type and loading condition (i.e., SENB specimens with side grooves to promote plane strain crack growth). The most significant finding in Figure 4 is that, when Δa is small the CTOA values are initially high, but progressively decrease to a nearly constant value. Note that in this experiment the fracture surface showed no evidence of tunneling. This finding may contradict a common speculation that the high CTOA values measured on the specimen surface at early stage of crack growth could be caused by the tunneling effect [5].

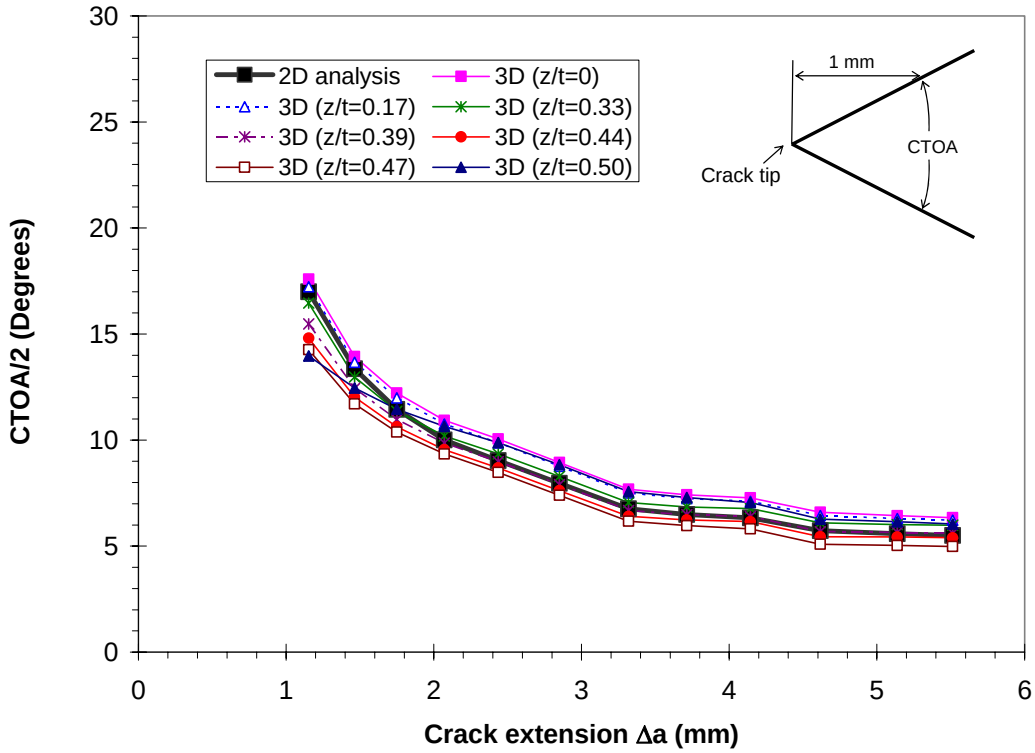

Figure 4 CTOA at 1 mm behind the crack tip vs. crack extension

Figure 5 summarizes the 3D-FEA results on the crack opening profile or CTOD at various locations behind the current crack tip. As the crack continues to grow, the CTOD progressively settles with a nearly constant crack opening profile. For any given crack extension (Δa), the value of CTOD depends on where the measurement takes place. At a specified distance from the current crack tip (e.g. 1 mm), this value is higher in the early crack growth phase and then decreases to a relatively constant CTOD as Δa increases. Therefore, it is important to recognize that 1) CTOD varies with the distance behind the crack tip; 2) CTOD varies with the amount of crack growth (Δa); and 3) CTOD fracture criteria should be reported and used with a specified distance from the crack tip.

Based on the results of the three- and two-dimensional analyses, it can be concluded that the stress state of these SENB specimens is predominantly plane strain. Therefore, the rest of the paper is focused on 2D-FEA. In addition, it was shown that the feature of non-constant CTOD in the early stage of crack growth is a common result for both two- and three-dimensional analyses, even when the crack tunneling effect is absent (experimentally and numerically). This feature is not a local phenomenon and is regardless of the location of measurement along the crack front across the specimen thickness.

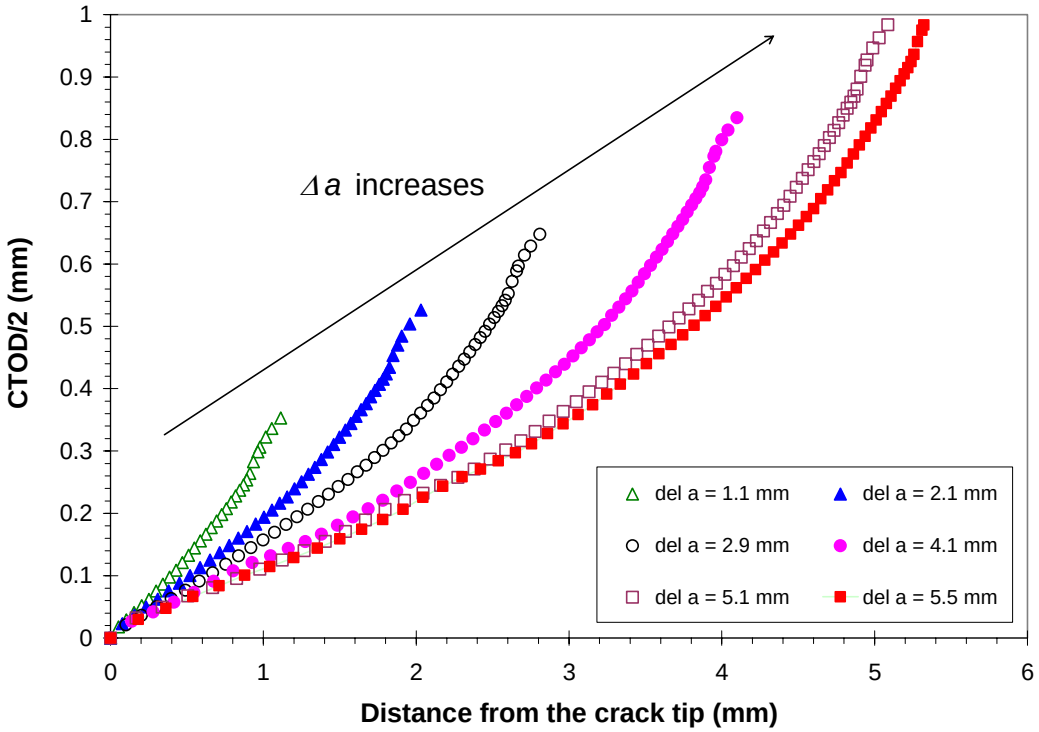

Figure 5 Comparison of the crack opening profiles calculated with 3D-FEA at the mid-plate of the SENB specimen

CTOD/CTOA FRACTURE CRITERIA

The numerical analysis in this paper consists of two parts. The goal of the first part of the analysis is to establish the CTOD as a function of crack growth (Δa), based on the experimental input of crack extension vs. load point displacement curve. The second part of analysis is to evaluate the performance of the CTOD fracture criteria based on the CTOD values calculated from the first part of analysis.

The CTOD values for a/W= 0.59 at 0.25, 0.5, and 1.0 mm behind the current crack tip are calculated in the first part of 2D-FEA and are plotted in Figure 6. It can be seen that the initial CTOD values are relatively high and then progressively decrease to a nearly constant value. Consequently, two CTOD criteria are proposed for the second part of 2D-FEA:

1. Constant CTOD Criterion

The initially non-constant values of CTOD are ignored. This popular approach uses the constant part of CTOD as a fracture criterion. In this particular case for a/W= 0.59, the crack growth is simulated with the finite element method and with the critical value of CTOD set to 0.062 mm (see Fig. 6, which is obtained at 0.25 mm behind the crack tip).

2. Bilinear CTOD Criterion

A bilinear form of the fracture criterion is used. As the dashed lines shown in Figure 6, the initial, non-constant values of CTOD are taken into consideration. The first few data points of the CTOD measured at 0.25 mm behind the crack tip are arbitrarily chosen for least-square fitting, which gives CTOD= 0.24 mm at zero crack growth and CTOD= 0.062 mm when Δa= 1.74 mm. The constant part of CTOD is 0.062 mm when $\Delta a \geq 1.74$ mm.

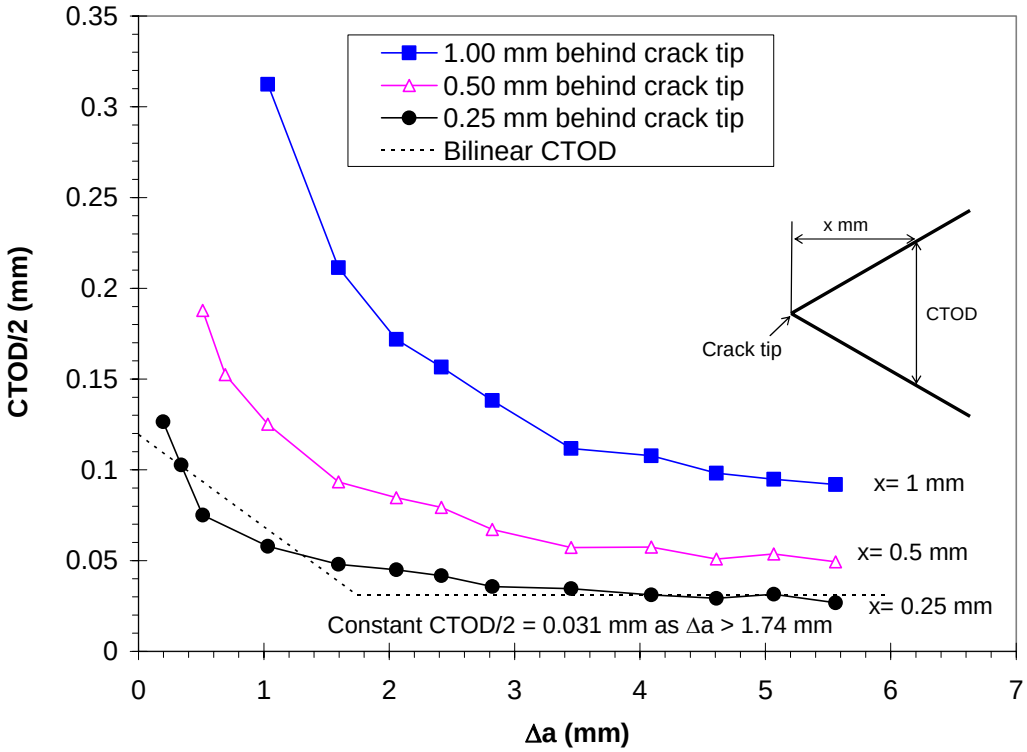

Figure 6 Calculated CTOD vs. crack extension for a/W = 0.59

As discussed earlier, the second part of the analysis involves the prediction of crack growth with a given CTOD criterion. With a constant CTOD fracture criterion (CTOD= 0.062 mm at 0.25 mm behind the current crack tip), the predicted load-displacement curve and the J-R curve are compared with the experimental data in Figures 7 and 8, respectively. It can be seen that this fracture criterion suffers a severe underestimation of the crack growth behavior. On the other hand, if the initial high value of CTOD is taken into consideration by using a simplified bilinear fracture criterion (Figure 6, dashed lines), the load-displacement and J-R curve can be recovered as shown in Figures 7 and 8. It can be seen that this simple bilinear fracture model works extremely well for predicting the crack growth behavior in the case of a/W= 0.59. Note that in this set of calculation, the CTOD criterion is referenced at 0.25 mm behind the current crack tip. If the criterion is given at another location from the crack tip (say, 1 mm), it is expected that the same conclusion can be made, that is, without the initial high values of CTOD, the crack growth prediction will be underestimated.

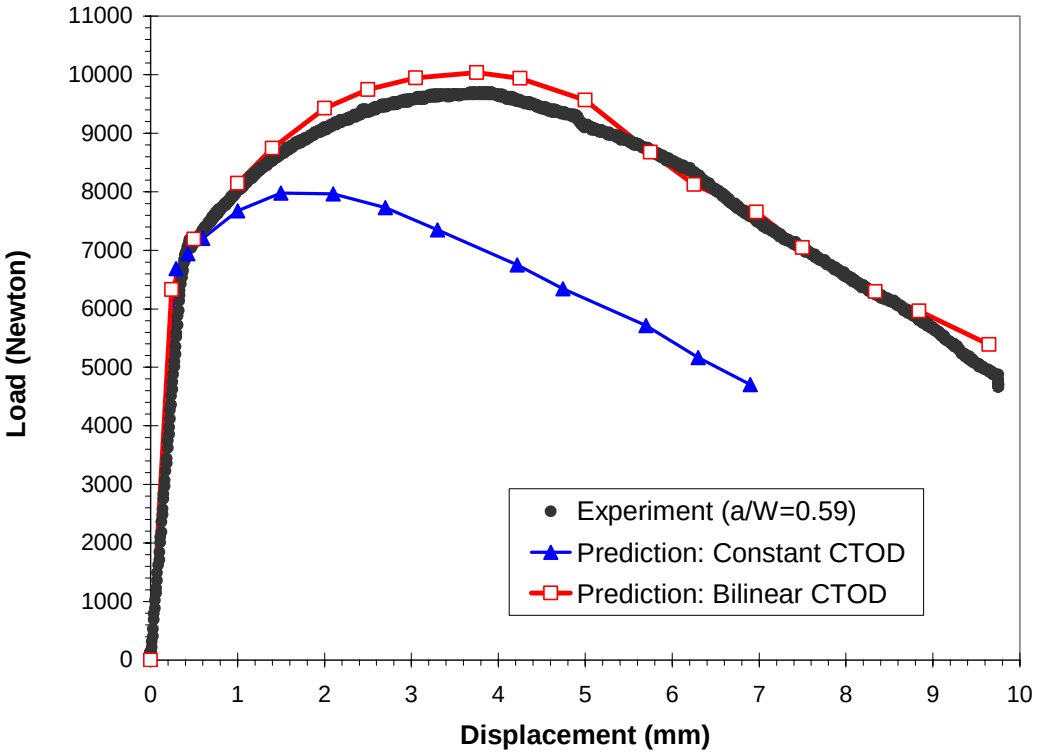

Figure 7 Comparison of predicted and experimental load-displacement curves for a/W= 0.59

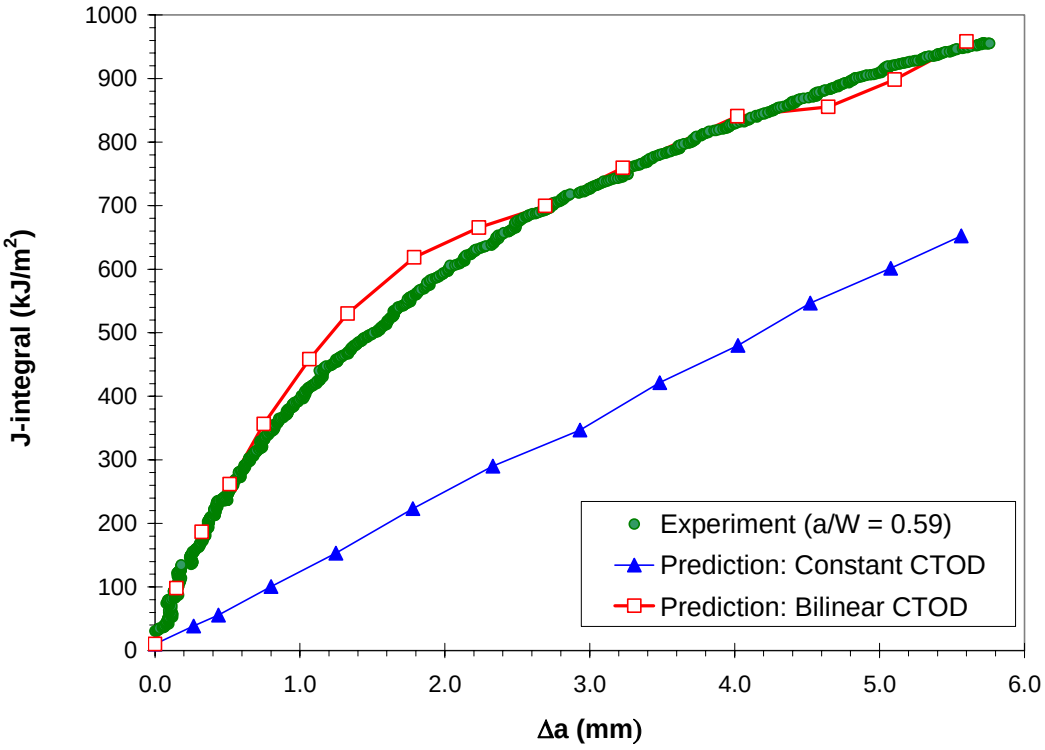

Figure 8 Comparison of predicted and experimental J-R curves for a/W= 0.59

NON-CONSTANT CTOD AND CONSTRAINT EFFECT

The non-constant CTOD is investigated in the context of crack tip constraint. Similar to the approach for the case of a/W =0.59, additional finite element analyses are performed for a high constraint specimen (a/W= 0.71) and for a low constraint specimen (a/W= 0.32). The J-R curves of these specimens (Fig. 2) clearly show the crack tip constraint effect and the material (A285 carbon steel) is capable of sustaining a large amount of stable crack growth. Similar to the case of a/W=0.59, the post-test fractography indicates that the crack fronts are relatively straight for all the specimens. Therefore, only plane strain analyses are considered for these two additional configurations.

Effect of Constraint on J-R Curve and CTOD

The finite element model for the high constraint specimen (a/W= 0.71) contains 13078 four-node elements with 13647 nodes. A similar model was designed for the low constraint case (a/W= 0.32) which has 13070 elements and 13631 nodes. A very fine, square mesh is placed around the crack tip and extends to the specimen edges for proper crack growth simulation and J-integral evaluation. The experimental curve of load-point displacement versus crack extension for each specimen is used as the fracture criterion to simulate crack growth and to calculate CTOD. As a result, the finite element calculated J-R curves (open symbols) are plotted against the experimental data in Figure 2. The good agreement again shows the adequacy of plane strain assumption and the numerical scheme. The constraint effect is obviously reflected by these J-R curves.

The CTOA values are calculated for these three specimens at a fixed distance of 1 mm behind the current crack tip. In Figure 9, it appears that each CTOA vs. Δa curve eventually approaches to a specific, but different, constant value. Apparently, these CTOA curves are functions of a/W, that is, crack tip constraint.

The importance of the initial, higher values of CTOD has been demonstrated in Figures 7 and 8. Without taking into consideration the non-constant portion of the fracture criterion, it would be detrimental for the subsequent prediction of crack growth. Attempts were made to use the bilinear CTOD criterion based on the case of a/W= 0.59 (Fig. 8) to predict the crack growth behavior for the cases of a/W=0.32 and 0.71, respectively. However, the prediction tends to overestimate the experimental data, but the results are superior to those obtained with a constant CTOD fracture criterion. Again, this implies that the CTOD is indeed constraint-dependent.

Since the simple bilinear form has demonstrated its viability in crack growth prediction for the case of a/W= 0.59, there is no compelling reasons to repeat the calculation for the cases of a/W= 0.71 and 0.32. From Figures 2 and 9, there is a clear connection between the crack tip constraint and the CTOD fracture criteria. For further

improvement in predicting crack growth, the constraint effect should be included in the development of fracture or crack growth criteria.

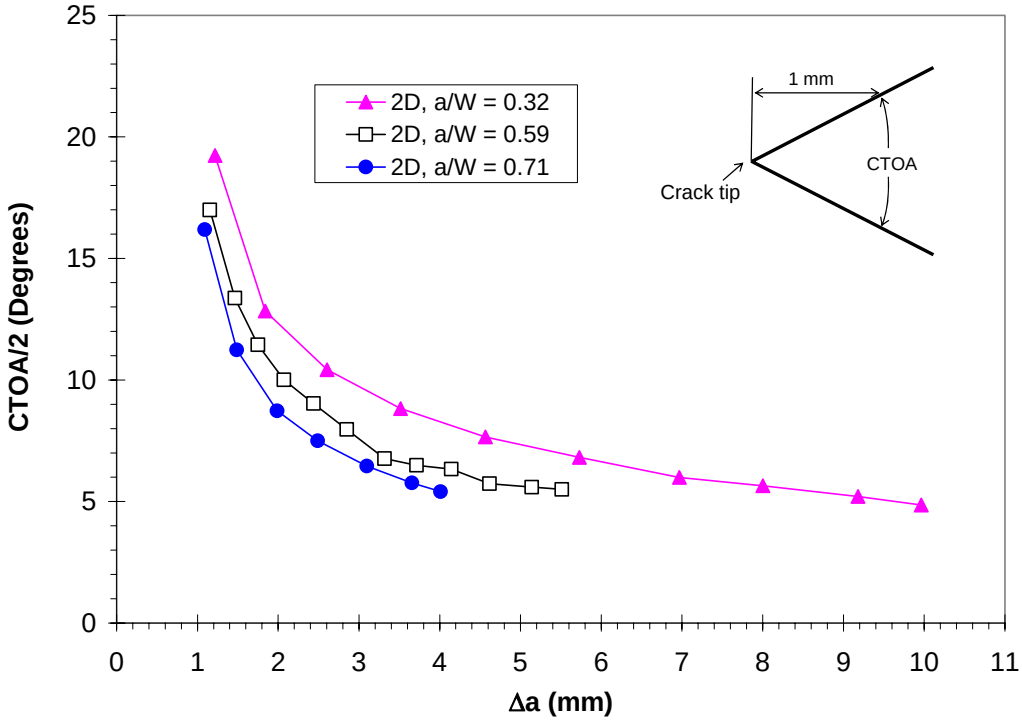

Figure 9 Comparison of CTOA for SENB specimens with various crack tip constraint

Theoretical Prediction of CTOD/CTOA

Using the Dougdale-Barenblatt strip yield model, the J-integral evaluation which utilizes the crack tip field solved by complex variable methods leads to a simple expression between J and CTOD (δ_t):

$$J = \sigma_y \delta_t \qquad (1)$$

where σ_y is a "generic" yield stress (as opposed to the 0.2% offset yield stress, σ_o). On the other hand, for a power law material characterized by Hutchinson-Rice-Rosengren (HRR) solution, and to define δ_t as the crack opening displacement between the intercepts of the two symmetric ±45° lines emanating from the deformed crack tip and the crack flange profile, it can be shown (e.g., [30]) that

$$J = \sigma_y \delta_t / d_n \qquad (2)$$

where d_n has been calculated by Shih [32] for cases of plane strain and plane stress, and is shown to be a strong function of strain hardening exponent (n) but weakly dependent of σ_y/E. For most engineering materials, $0 < d_n \leq 1$ for plane stress and $0 < d_n < 0.8$ for plane strain [30,31]. From Eq. (1) and more generally Eq. (2), Kanninen et al. [30] pointed out

that J and δ_t (or CTOD) are equivalent, and "any fracture criterion based upon a critical value of δ_t is equivalent to one based upon a critical value of J and vise versa." Of course, the HRR dominance must be satisfied in this aspect.

Equations (1) and (2) can be collectively expressed as [16]

$$J = m\sigma_y \delta_t \quad (3)$$

where m could be a constant for a specific material. By differentiation of Eq. (3) with respect to the crack length (a), with an additional approximation that m remains unchanged during (the limited amount of) crack extension, then the relationship between CTOA and the slope of the J-R curve (or tearing modulus) may be established as [16,33]:

$$CTOA = d\delta_t/da = (dJ/da)/(m\sigma_y) \quad (4)$$

It appears that the factor m can be obtained by experimental data if J-R curve is known and CTOA has been calculated or measured. However, practically speaking, the factor m may not be exactly a constant due to the fluctuation of the experimental data points, and it may somehow depend on the crack tip constraint. For demonstration purpose, the value of m is solved by using the first data point in Figure 9 and the experimental J-R curve for each specimen. Because Eq. 4 is very sensitive to the local slope, sampling data points were selected from the J-R curves in Figure 2. In addition, the slope between any two sampling points is assumed to be a constant. To take strain hardening into consideration, the flow stress of this material (σ_f= 333 MPa) is used in place of σ_y. The values of m derived from this process are 1.27, 1.16, and 1.01, respectively, for specimens with a/W of 0.32, 0.59, and 0.71. The predicted CTOA as a function of Δa can be seen in Figure 10, on which the data points used in Figure 9 are superimposed for comparison. A qualitative agreement is achieved between the finite element-calculated CTOA and the prediction based on experimental J-R curves. Therefore, the initial high values of CTOD/CTOA are indeed a natural consequence of the crack growth resistance as reflected by the J-R curve.

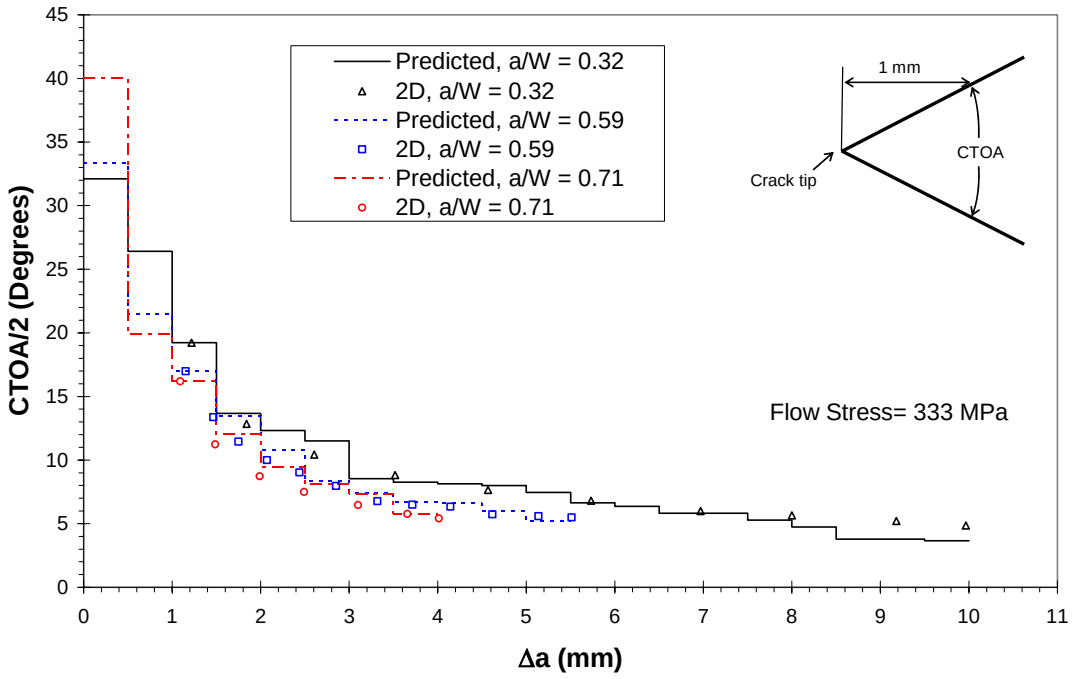

Figure 10 Theoretical and numerical predictions of CTOA based on J-R curves

CONCLUDING REMARKS

The SENB specimens with various a/W ratios were previously tested for developing a constraint-modified J-R curve [25]. The crack growth dada obtained from that set of J-R test are used to investigate the CTOD-based fracture criteria. The fractography of the post-test specimens showed that the crack fronts are straight. The crack tunneling is eliminated as an influential factor in this study. Both three- and two-dimensional finite element analyses are performed to simulate the ASTM E 1820 J-integral testing. The similarity of these finite element solutions confirms that the deformation is essentially plane strain, and the two-dimensional analysis is adequate for the determination of CTOD during the crack growth. Subsequently, the plane strain analysis is employed along with the CTOD fracture criterion to conversely predict the J-integral. Very good agreement was achieved between the predicted and the experimental J-R curves.

The current investigation shows that CTOD can be related to the J-integral/tearing modulus, at least for power law (HRR) materials [29,30,33] and for the perfectly plastic materials [16,34]. This relationship analytically leads to higher CTOD values in the beginning of crack growth, and then progressively decreases to a nearly constant value for most of the materials that exhibit typical J-R curves. This is a common feature of the CTOA that can be seen from the literature data [6-10] (collectively reported by Newman

et al. [5]). Since it is well known that the J-R curve is specimen configuration dependent, it can be concluded that the CTOD may strongly depend on crack tip constraint.

As shown in this paper, the initial higher values of CTOD are essential in predicting crack growth in specimens under predominantly plane strain conditions. Without including the initial values, the crack growth behavior is severely underestimated (Figs. 7,8). However, The functional dependence between the CTOD and the constraint parameters such as A_2 [26-28], T [35], or Q [36,37], has not been fully established. O'Dowd [38] developed a constraint-dependent d_n (see Eq. 2) for a power law material (n= 10) based on a stationary crack solution, which is expected to be valid, at least, for small amount of crack extension. However, the CTOD in that case is still defined by the two 45° lines emanating from the crack tip. For crack opening angle less than 90°, the application is probably limited. The key to overcome this difficulty seems to rest on the development of a complete solution which, in particular, must be valid in the area immediately behind the advancing crack tip where unloading is known to take place [39-44].

Acknowledgment

G. K. Chapman and Dr. M. J. Morgan of Savannah River National Laboratory (SRNL) are greatly appreciated for conducting the SENB fracture testing. PSL acknowledges the support from the United States Department of Energy (DOE) Office of Science Environmental Management Science Program (EMSP), and from SRNL/Savannah River Site (SRS) High Level Waste Division under the Independent R&D Program, funded by DOE under Contract No. DE-AC09-96SR18500. YK and YJC were supported by the U. S. National Science Foundation grant CMS0116238 and partially by DOE through the South Carolina Universities Research and Education Foundation (SCUREF).

References

[1] Mahmoud S, Lease K. The effect of specimen thickness on the characterization of critical CTOA in 2024-T351 aluminum alloy, Engng Fract Mech 2003;70:443-56.
[2] Luo PF, Chao YJ, Sutton MA, Application of stereo vision to 3D deformation analysis in fracture mechanics, Optical Engineering 1994;33(3):981-990.
[3] Chao YJ, Sutton MA. Accurate measurement of two- and three-dimensional surface deformations for fracture specimens by computer vision: Experimental Techniques in Fracture; ed. Epstein JS, VCH Publisher 1993;59-94.
[4] Lloyd WR. Microtopography for ductile fracture process characterization: Part 1: Theory and methodology, Engng Fract Mech 2003;70:387-401.
[5] Newman Jr JC, James MA, Zerbst U. A review of the CTOA/CTOD fracture criterion. Engng Fract Mech 2003;70:371-85
[6] Shih CF, de Lorenzi HG, Andrews WR. Studies on crack initiation and stable crack growth. ASTM STP 1979;668:65–120.

[7] Kanninen MF, Rybicki EF, Stonesifer RB, Broek D, Rosenfield AR, Nalin GT. Elastic–plastic fracture mechanics for two dimensional stable crack growth and instability problems. ASTM STP 1979;668:121–50.
[8] Brocks W, Yuan H. Numerical studies on stable crack growth. In: Defect Assessment in Components Fundamentals and Applications, vol. 9. ESIS Publication; 1991:19–33.
[9] Newman Jr JC, Shivakumar KN, McCabe DE. Finite element fracture simulation of A533B steel sheet specimens. In: Defect Assessment in Components Fundamentals and Applications, 9. ESIS Publication; 1991:117–26.
[10] James MA, Newman Jr JC. Three-dimensional analyses of crack-tip-opening angles and δ5-resistance curves for 2024-T351 aluminum alloy. ASTM STP 2002;1406:279–97.
[11] Newman Jr JC, Booth BC, Shivakumar KN. An elastic–plastic finite-element analysis of the J-resistance curve using a CTOD criterion. ASTM STP 1988;945:665–85.
[12] Newman Jr JC, Dawicke DS, Bigelow CA. Finite-element analyses and fracture simulation in thin-sheet aluminum alloy. In: Durability of Metal Aircraft Structures. Georgia: W.H. Wolfe Associates; 1992:167–86.
[13] Dawicke DS, Sutton MA. CTOA and crack tunneling measurements in thin sheet 2024-T3 aluminum alloy. Exp Mech 1994;34(4):357.
[14] Dawicke DS, Piascik RS, Newman JC, Jr. Analysis of stable tearing in a 7.6 mm thick aluminum plate alloy, Fatigue and Fracture Mechanics: 28th Volume, *ASTM STP 1321*, American Society for Testing and Materials 1997:309-324.
[15] Dawicke DS, Sutton MA, Newman Jr JC, Bigelow CA. Measurement and analysis of critical CTOA for an aluminum alloy sheet. ASTM STP 1999;1220:358–79.
[16] Gullerud AS, Dodds Jr RH, Hampton RW, Dawicke DS. Three-dimensional modeling of ductile crack growth in thin sheet metals: computational aspects and validation. Engng Fract Mech 1999;63:347–74.
[17] Hampton RW, Nelson D, Stable crack growth and instability prediction in thin plates and cylinders. Engng Frac Mech 2003:469-491.
[18] Mahmoud S, Lease K. Two-dimensional and three-dimensional finite element analysis of critical crack-tip-opening angle in 2024-T351 aluminum alloy at four thicknesses. Engng Fract Mech 2004;71:1379-91.
[19] Shterenlikht A, Hashemi SH, Howard IC, Yates JR, Andrews RM, A specimen for studying the resistance to ductile crack propagation in pipes, Engng Frac Mech 2004;71:1997-2013.
[20] Shivakumar KN, Newman Jr JC. ZIP3D—An elastic and elastic–plastic finite-element analysis program for cracked bodies, NASA TM 102753, 1990.
[21] James MA, Residual strength calculations for single and multiple-site damage cracks. First Joint DoD/FAA/NASA Conference on Aging Aircraft, July 1997;1789–802.
[22] James MA, Newman Jr JC. Importance of crack tunneling during fracture: experiments and CTOA analyses, 10th International Congress of Fracture, Honolulu, Hawaii, December 3–7, 2001.
[23] Koppenhoefer KC, Gullerud AS, Ruggieri C, Dodds Jr RH. WARP3D: Dynamic nonlinear analysis of solids using a preconditioned conjugate gradient software architecture, Structural Research Series 596, UILU-ENG-94-2017, University of Illinois, 1994.

[24] ABAQUS Standard, ABAQUS Inc., Pawtucket, RI.
[25] Lam PS, Chao YJ, Zhu XK, Kim Y, Sindelar RL. Determination of Constraint-Modified J-R Curves for Carbon Steel Tanks. J Press Vessel Tech 2003;125:136-43.
[26] Yang S, Chao YJ, Sutton MA. Higher order asymptotic crack tip fields in a power-law hardening material. Engng Fract Mech 1993;45:1-20.
[27] Yang S, Chao YJ, Sutton MA. Complete theoretical analysis for higher order asymptotic terms and the HRR zone at a crack tip for mode I and Mode II loading of a hardening material. ACTA MECHANICA 1993;98:79-98.
[28] Chao YJ, Yang S, Sutton MA. On the fracture of solids characterized by one or two parameters: theory and practice. J Mech Phys Solids 1994;42:629-47.
[29] Kanninen MF et al. Development of a Plastic Fracture Methodology. EPRI NP-1734, Project 601-1, Final Report, March 1981.
[30] Kanninen MF, Popelar CH. Advanced Fracture Mechanics. Oxford University Press 1985.
[31] Lloyd WR, McClintock FA. Microtopography for ductile fracture process characterization: Part 2: Application for CTOA analysis, Engng Fract Mech 2003;70: 403-15.
[32] Shih CF, Relationship between the J-integral and the crack displacement for stationary and extending cracks, J. Mech. Phys. Solids 1981:29:305-26.
[33] Omidvar B, Wnuk M, Choroszynski, Relationship between the CTOD and the J-integral for stationary and growing cracks: Close form solutions, Int. J. Fract 1997; 87:331-43.
[34] Anderson TL. Fracture Mechanics: Fundamentals and Applications 2nd Ed. CRC Press, 1995.
[35] Betegon C, Hancock JW, Two parameter characterization of elastic-plastic crack-tip fields, J. Appl. Mech. 1991; 58:104–10.
[36] O'Dowd NP, Shih CF. Family of crack-tip fields characterized by a triaxiality parameter - I. Structure of fields, J. Mech. Phys. Solids 1991;39:989–1015.
[37] O'Dowd NP, Shih CF. Family of crack-tip fields characterized by a triaxiality parameter - II. Fracture applications, J. Mech. Phys. Solids 1992; 40:939–63.
[38] O'Dowd NP. Applications of two parameter approaches in elastic-plastic fracture mechanics, Engng Fract Mech 1995;52: 445-65.
[39] Rice JR, Drugan WJ, Sham TL. Elastic-plastic of growing cracks. ASTM STP 1980;700:189-221.
[40] Dean R, Hutchinson JW. Quasi-static steady crack growth in small scale yielding, ASTM 1980;700:383-405.
[41] Parks DM, Lam PS, McMeeking RM. Some effects on inelastic constitutive models on crack tip fields in steady quasistatic growth. Advances in Fracture Research 1981; 5:2607-14.
[42] Lam PS. Numerical analysis of stable crack growth in elastic-plastic materials in small scale and general yielding. UILU-ENG 82-6003 1982; Univ. of Illinois T&AM Report No. 455.
[43] Lam PS, McMeeking RM. Analysis of steady state quasistatic crack growth in plane strain tension in elastic-plastic materials with non-isotropic hardening. J Mech Phys Solids 1984;32: 395-414.

[44] Lam PS, Freund LB. Analysis of dynamic growth of a tensile crack in an elastic-plastic material. J Mech Phys Solids 1985;33: 153-67.